The conductivity of Bi(111) investigated with nanoscale four point probes

Wells, J.W.; Handrup, K.; Kallehauge, J.F.; Gammelgaard, Lauge; Bøggild, Peter; Balslev, Mette Bjerrum; Hansen, J.E.; Petersen, P.R.E.; Hofmann, P.

Published in:
Journal of Applied Physics

Link to article, DOI:
10.1063/1.2969769

Publication date:
2008

Document Version
Publisher's PDF, also known as Version of record

The conductivity of Bi(111) investigated with nanoscale four point probes

J. W. Wells,[1,a)] K. Handrup,[1] J. F. Kallehauge,[1] L. Gammelgaard,[2] P. Bøggild,[2] M. B. Balslev,[3] J. E. Hansen,[3] P. R. E. Petersen,[3] and Ph. Hofmann[1,b)]
[1]*Institute for Storage Ring Facilities (ISA) and Interdisciplinary Nanoscience Center (iNANO), University of Aarhus, 8000 Aarhus C, Denmark*
[2]*Department of Micro- and Nanotechnology, Technical University of Denmark, 2800 Kgs. Lyngby, Denmark*
[3]*Capres A/S, 2800 Kgs. Lyngby, Denmark*

(Received 13 February 2008; accepted 17 May 2008; published online 10 September 2008)

The room temperature conductance of Bi(111) was measured using microscopic four point probes with a contact spacing down to 500 nm. The conductance is remarkably similar to that of the bulk, indicating that surface scattering is not a major mechanism for restricting the mobility at this length scale. Also, the high density of electronic surface states on Bi(111) does not appear to have a major influence on the measured conductance. The lower limit for the resistivity due to electronic surface states is found to be around 5 Ω. With such a value for the surface resistivity, surface conduction should not be a significant factor to inhibit the observation of the predicted semiconductor to semimetal transition for thin films of Bi. © *2008 American Institute of Physics*.
[DOI: 10.1063/1.2969769]

I. INTRODUCTION

Bismuth is a group V semimetal with a very low density of states at the Fermi level, about five orders of magnitude lower than that of a typical metal such as copper.[1] The Fermi surface consists of small electron and hole pockets at the *L* and *T* points of the Brillouin zone. The Fermi energy for the electrons and holes is small, in the order of 25 meV, and the effective masses of the carriers are highly anisotropic and small (down to one-hundredth of an electron mass). As a consequence of this, the carriers have a very long de Broglie wavelength and high mobility. This leads to pronounced quantum size effects in thin films, which were first observed for Bi.[2]

Soon after the discovery of quantum size effects, it was argued that the overlap of valence and conduction bands should vanish altogether for films with a thickness of less than approximately 20–30 nm,[3,4] and the semimetal should hence turn into a semiconductor. More than 30 years after this prediction and after considerable experimental and theoretical effort (see for example Refs. 5–9 and references therein), it remains unclear if this transition takes place or not.

One important factor in these experiments appears to be the quality of the films. In most studies, the films were observed to show *p*-type conductivity and, only recently, *n*-type behavior was found in high quality films,[10] which even showed quantum size effects at room temperature. If film quality is an issue, it is likely that defect-induced carriers could prevent the clear observation of the semimetal to semiconductor transition.

It was, of course, realized early on that the most important and unavoidable "defect" in a thin film is the surface or the interface to the substrate. These two interfaces set up the boundary condition for the quantum states and they can also support localized electronic states at the Fermi level, which could dominate the transport properties of a sufficiently thin film.[5,6,8]

Later, it was indeed found that many low-index surfaces of Bi studied are good two dimensional metals[11–14] (for a review see Ref. 15) in the sense of supporting metallic surface states which increase the density of states at the Fermi level. This strong difference between bulk Bi and its surfaces is not merely a consequence of the different atomic coordination but of the symmetry breaking at the surface and the strong spin-orbit interaction in Bi.[16,17] It can be expected to be a universal feature of Bi surfaces. Consistent with this, the presence of metallic surface states on Bi clusters and nanowires has been discussed.[18,19]

Given the existence of electronic surface states and their possible role in preventing an observation of the semimetal to semiconductor transition, an interesting question to ask is how much the surface states would influence the transport properties of the sample. In the present paper, we address this problem by probing the conductance of Bi(111) using a newly developed nanoscale four point probe.[20] Four point probes have successfully been used to determine the surface conductance of semiconductor surfaces for cases where the conductance of the space charge layer and the bulk are negligible compared to that of the surface.[21–24]

If the goal of the experiment is to determine the conductance due to the surface states of Bi, the best approach for doing this is to use a Bi single crystal as a sample, not a thin film with concomitant problems of quantum size effects and carriers induced at the film-substrate interface. We therefore performed our measurements on the (111) surface of Bi for which the electronic structure and even the lifetime of the surface states are well known.[12–26] (111) is also the preferred

[a)]Electronic mail: jwells@phys.au.dk.
[b)]Electronic mail: philip@phys.au.dk. Present address: Surface Science Research Centre, University of Liverpool, Liverpool L69 3BX, United Kingdom.

growth direction for thin films. Our findings have direct relevance for the study of the semimetal to semiconductor transitions in these films.

Surface sensitivity in conductance measurements can be achieved by using very small collinear four point probes. This is because the measured four point probe resistance (i.e., the voltage drop over the inner two contacts divided by the current through the outer contacts) does not depend on the contact spacing for a two dimensional sheet but for a semi-infinite bulk. More precisely, the measured resistance for a two-dimensional sheet is

$$R_{2D}^{4pp} = \frac{\ln 2}{\pi \sigma_s}, \tag{1}$$

where σ_s is the sheet conductivity. Note that the unit of σ_s is merely Ω^{-1}, not $\Omega^{-1}\ m^{-1}$ as in the case for bulk conductivity. For a semi-infinite bulk, on the other hand, one obtains

$$R_{3D}^{4pp} = \frac{1}{2\pi s \sigma_b}, \tag{2}$$

with the bulk conductivity as σ_b and the contact spacing as s.[27] If we adopt the simple view that the surface and the bulk of a solid behave as two parallel resistors with R_{2D}^{4pp} and R_{3D}^{4pp}, respectively, it follows that nearly the entire current will pass through the surface only if s is sufficiently small. Being able to change s would obviously be advantageous to single out surface and bulk contributions from a measurement. Using nonequidistant contact distances can also be of advantage; an approach to the data analysis for this will be presented later in this paper.

II. EXPERIMENTAL

The measurements were made on a Bi(111) sample acquired from Mateck GmbH. The surface was mechanically and electrochemically polished before insertion into ultrahigh vacuum. The surface was prepared *in situ* by cycles of Ar^+ ion bombardment at 500 eV, followed by annealing to 150 °C. The surface order and cleanliness were confirmed using low energy electron diffraction.

The conductivity measurements were performed using a prototype monocantilever probe from Capres A/S.[28] The probe consists of a single SiO_2 cantilever, onto which 12 metallic wires are patterned at varying distances from each other. These metallic wires form the contact to the sample surface. Any four of these can be used for the conductance measurements such that a very large variety of contact spacing is possible. Details of the probe construction can be found in Ref. 20.

The probes are positioned in vacuum using piezomotors and the approach to the surface is controlled using the image from an optical microscope. In this way, the position of the probe can be controlled with submicron precision.

After contacting the surface, a current is directed between each contact and the sample substrate, thus allowing each contact resistance to be measured. The pressure of the probe on the surface can be adjusted such that reliable contacts are formed. A four point measurement is then made by increasing the current flowing through two of the contacts

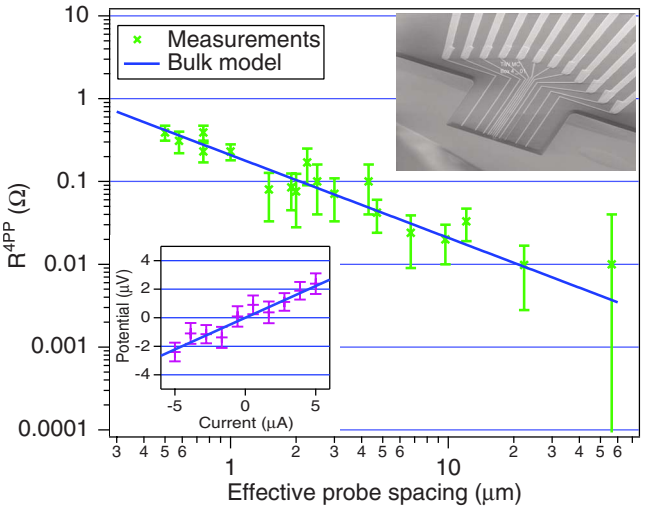

FIG. 1. (Color online) The measured four point resistance vs the effective contact spacing. The solid blue line indicates the expected resistance for bulk Bi (using $\rho_{bulk} = 1.3 \times 10^{-6}\ \Omega$ m after Ref. 29) A picture of the probe and an *I-V* curve (measured using a contact spacing of 500 nm) are shown in the insets.

(usually the outermost two) while measuring the potential drop over the remaining two contacts (so-called *I-V* measurement). Typically, the current is linearly increased from −5 to +5 μA over a period of about 20 s. After such a measurement, the current is immediately decreased again so that the same measurement can be made using a negative current ramp. By doing this, any charging effects become apparent and the ramp time can be adjusted to eliminate this if necessary. Each measurement is repeated many times such that the signal to noise ratio is improved. Typically this requires 100 independent sweeps. Further details of the probes with the ultrahigh vacuum instrument and measurement procedure can be found elsewhere.[20,23,24]

In order to vary the contact spacing, two different techniques are employed. First, since each monocantilever probe has 12 contacts and since only 4 are required to perform the conductivity measurement, the contact spacing can be changed by simply selecting different contacts. This allows the spacing between the contacts to be varied over about an order of magnitude depending on the design of the 12 point probe (the positions of the contacts on a typical 12 contact monocantilever can be seen in the inset of Fig. 1). Second, a variety of probe designs have been produced by Capres A/S, so an even wider range of spacings can be achieved by exchanging the probe for one with an alternative contact layout. In this work, both methods are employed. Four different probe designs are used, which allows us to vary contact spacings from 500 nm to 56 μm.

Given the opportunity to work with nonequal contact spacings, Eq. (2) has to be generalized to allow for this possibility. This results in

$$R_{3D}^{4pp} = \frac{1}{2\pi\sigma_b}\left(\frac{1}{s_{12}} + \frac{1}{s_{34}} - \frac{1}{s_{23}+s_{34}} - \frac{1}{s_{12}+s_{23}}\right), \tag{3}$$

where s_{nm} denotes the spacing between contact numbers n and m. To facilitate a comparison with the case of equal spacings and to allow a meaningful presentation of data, one

can define an *effective spacing* (s_{eff}) as

$$\frac{1}{s_{\text{eff}}} = \frac{1}{s_{12}} + \frac{1}{s_{34}} - \frac{1}{s_{12}+s_{23}} - \frac{1}{s_{23}+s_{34}}. \tag{4}$$

III. RESULTS AND DISCUSSION

The resistance, and the corresponding uncertainty, is extracted from the *I-V* measurements by means of a linear fit weighted according to the standard deviation of the individual data points. In all cases, the linear fit is justified by the Ohmic nature of the measured four point resistance. An example *I-V* curve (from the data taken with a 500 nm contact spacing) is shown in the inset of Fig. 1. As with all the *I-V* curves, it is linear within this current range. The value of the resistance, as extracted from the *I-V* curves, versus the effective spacing is plotted in Fig. 1.

When the four point resistance is relatively large, so is the measured potential (i.e., in the order of microvolts), and since this is also large relative to the stray electrical noise, the uncertainty in the measurement is small. Conversely, when the four point resistance is small, the uncertainty in the measurement increases significantly. This is apparent in Fig. 1.

The data presented in Fig. 1 were collected using several different probes and after subsequent preparations of the surface. Despite this, the measurements show no significant deviation from the general trend.

Figure 1 also shows the expected four point resistance for bulk Bi. The data are relatively well represented by this bulk-only model, even at the smallest spacing of only 500 nm. From this we can conclude that scattering of bulk carriers at the surface is fairly insignificant. The penetration of the current into the sample is of the same order of magnitude as the spacing between the contacts such that the current density for the smallest contact spacing is strongly localized near the surface. Even so, the accompanying reduction in carrier mobility appears to be small. Hence, one would also expect surface scattering for a well-ordered thin film to be small.

Plotting the data as in Fig. 1 allows us to draw the inference that the surface contribution is not significant since the data are generally well described by the bulk model. However, to include a surface contribution in the model is not straightforward because of the choice of the effective spacing for the horizontal axis. This is because, in order to calculate the effective spacing using Eq. (4), one tacitly assumes that bulk-sensitive measurements are performed. Thus, in order to demonstrate the influence of a surface contribution, it is necessary to choose a parameter for the horizontal axis that does not involve such an assumption.

An appropriate alternative approach is to treat the bulk and the surface as two parallel resistors. In order to do this, we have to investigate the effect of unequal probe spacings on the measured resistance for a two-dimensional sheet as well, i.e., we will have to find a generalization of Eq. (1) in the same way as for Eq. (2). The solution is no longer independent of the contact spacings but rather takes the form

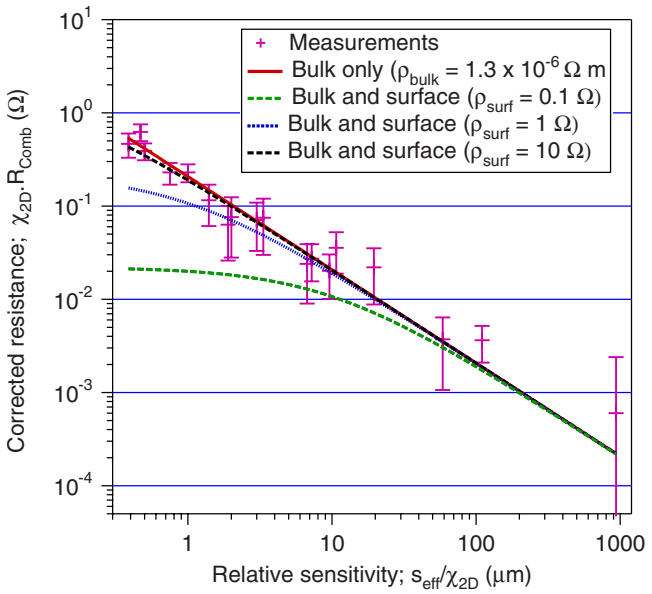

FIG. 2. (Color online) The measured four point resistance (corrected and incorporating the surface sensitivity) plotted against the relative sensitivity s_{eff}/χ_{2D}. The solid line indicates the expected behavior for a bulk dominated measurement. The black dashed lines indicate the expected behavior for the combined bulk and surface terms (using surface resistivities of 0.1, 1, and 10 Ω).

$$R_{2D}^{4pp} = \frac{1}{2\pi\sigma_s}\left(\ln\frac{s_{23}+s_{34}}{s_{12}} + \ln\frac{s_{12}+s_{23}}{s_{34}}\right). \tag{5}$$

In order to relate Eq. (5) with Eq. (1) in a simple way, it is useful to introduce *surface sensitivity* χ_{2D},

$$\frac{1}{\chi_{2D}} = \frac{1}{2\ln 2}\left(\ln\frac{s_{23}+s_{34}}{s_{12}} + \ln\frac{s_{12}+s_{23}}{s_{34}}\right). \tag{6}$$

Thus Eq. (5) can be expressed more succinctly as

$$R_{22D}^{4pp} = \frac{1}{\chi_{2D}}\frac{\ln 2}{\pi\sigma_s}. \tag{7}$$

Combining Eqs. (3), (4), and (7) by treating surface and bulk as two parallel resistors yields

$$\chi_{2D}R_{\text{comb}}^{4pp} = \frac{1}{2\pi\sigma_b\, s_{\text{eff}}/\chi_{2D} + \pi\sigma_s/\ln 2}. \tag{8}$$

This equation is arranged such that the right hand side contains only the conductivities and the quantity s_{eff}/χ_{2D}. We now call s_{eff}/χ_{2D} the *relative sensitivity* since low values indicate surface sensitivity and high values indicate bulk sensitivity.

According to Eq. (8), a good way to display data containing surface and bulk contributions obtained with non-equidistant contact spacings is to plot $\chi_{2D}R_{\text{comb}}^{4pp}$ as a function of the relative sensitivity. This is done in Fig. 2 together with calculations assuming a pure bulk behavior or a combination of bulk and surface conductances. An inspection of the different calculations shows that a low surface resistivity (such as 0.1 Ω) can definitely be excluded and that the surface resistivity must be at least ≈5 Ω.

It is interesting to estimate the order of magnitude one could expect for the surface state resistivity by using differ-

ent assumptions for the mobility. If we are only interested in an order of magnitude estimate, we can use the following numbers: The carrier density of the surface states (electrons and holes) is in the order of $d=10^{13}$ cm^{-2}, their effective masses m^* are in the order of one electron mass,[12,25] and the room-temperature lifetime of the electrons near the Fermi level $\tau(E_F)$ is of the order of 5 fs.[26]

The first estimate for the surface state resistivity can be made assuming that the specific surface electronic structure increases the number of carriers but the mobility of these carriers is that of the bulk.[30] These assumptions result in a small surface resistance of 6 Ω, just at the limit of what could be detected in the present experiment. An alternative approach would be to take the observed room temperature mobility in a thin film[8] which would lead to a surface resistivity of 600 Ω.

A more sensible estimate of the surface resistivity, however, would be based on not taking any value for the bulk mobility but using the measured surface state lifetime value.[12,25] Indeed, using the bulk mobility will almost certainly lead to a strong underestimate of the surface resistivity because this mobility is strongly influenced by the small effective masses of the carriers in Bi. Instead, we can estimate the order of magnitude of the surface resistivity by a simple Drude model, i.e.,

$$\rho = \frac{m^*}{de^2\,\tau(E_F)}, \tag{9}$$

which, with the values given above, gives $\rho=71$ kΩ, a high value which could not be measured with any realistically sized four point probe.

IV. CONCLUSIONS

The most important result of this study is that the presence of electronic surface states and the conduction through these states is a very unlikely source for the experimental problems in finding the semimetal to semiconductor transition in thin Bi films. Even though there is some experimental uncertainty in the resistivity of a 20–30 nm film,[10,31,32] the surface state contribution to the conductance will be insignificant. The physical reason for this is not the special character of the surface states but the unusual bulk. Due to the small effective masses and the high mobility of the bulk carriers, the transport through the bulk will be dominant. Our study has also shown that a high quality surface will not even give rise to strong scattering and a pronounced reduction in mobility. The surface probably has a resistance of many hundreds or thousands of ohms. This can be expected to be a typical value for a surface resistance; even if the surface supports a high carrier density and a "normal" mobility, the absolute number of these carriers is still small.

If the surface states are not responsible for inhibiting the semimetal to semiconductor transition, what is? A critical issue appears to be the film quality. Recent results have shown that this strongly matters and that high quality films can show *n*-type conductance and even quantum size effects at room temperature.[10] A promising path toward high quality films appears to be growing these films on Si(111).[33–35]

Since preparing this manuscript, we have become aware of the study by Hirahara *et al.*,[36] in which measurements of the conductivity of thin Bi films on Si(111) are presented. In this work, the surface state conductance for Bi(111) is reported as $\approx 1.5\times10^{-3}\ \Omega^{-1}$ at room temperature. Such a value is consistent with our measurements.

ACKNOWLEDGMENTS

This project was funded by the Danish Ministry of Science, Technology and Innovation through the MiNaP innovation consortium. P.H. thanks the Leverhulme Foundation for supporting a stay at the University of Liverpool.

[1] V. S. Édel'man, Adv. Phys. **25**, 555 (1976).
[2] Y. F. Ogrin, V. N. Lutskii, and M. I. Elinson, JETP Lett. **3**, 71 (1966).
[3] V. N. Lutskii, Sov. Phys. JETP **2**, 245 (1965).
[4] V. B. Sandomirskii, Sov. Phys. JETP **25**, 101 (1967).
[5] Y. F. Komnik, E. N. Bukhshtab, Y. V. Nikitin, and V. V. Andrievskii, Zh. Eksp. Teor. Fiz. **60**, 669 (1971).
[6] Y. F. Komnik and V. V. Andrievskii, Fiz. Nizk. Temp. **1**, 104 (1975).
[7] H. T. Chu, P. N. Henriksen, and J. Alexander, Phys. Rev. B **37**, 3900 (1988).
[8] C. A. Hoffman, J. R. Meyer, F. J. Bartoli, A. D. Venere, X. J. Xi, C. L. Hou, and H. C. Wang, Phys. Rev. B **48**, 11431 (1993).
[9] H. T. Chu, Phys. Rev. B **51**, 5532 (1995).
[10] E. I. Rogacheva, S. N. Grigorov, O. N. Nashchekina, S. Lyubchenko, and M. S. Dresselhaus, Appl. Phys. Lett. **82**, 2628 (2003).
[11] S. Agergaard, C. Søndergaard, H. Li, M. B. Nielsen, S. V. Hoffmann, Z. Li, and P. Hofmann, New J. Phys. **3**, 15.1 (2001).
[12] C. R. Ast and H. Höchst, Phys. Rev. Lett. **87**, 177602 (2001).
[13] P. Hofmann, J. E. Gayone, G. Bihlmayer, Y. M. Koroteev, and E. V. Chulkov, Phys. Rev. B **71**, 195413 (2005).
[14] K. Sugawara, T. Sato, S. Souma, T. Takahashi, M. Arai, and T. Sasaki, Phys. Rev. Lett. **96**, 046411 (2006).
[15] P. Hofmann, Prog. Surf. Sci. **81**, 191 (2006).
[16] Y. M. Koroteev, G. Bihlmayer, J. E. Gayone, E. V. Chulkov, S. Blügel, P. M. Echenique, and P. Hofmann, Phys. Rev. Lett. **93**, 046403 (2004).
[17] J. I. Pascual, G. Bihlmayer, Y. M. Koroteev, H. P. Rust, G. Ceballos, M. Hansmann, K. Horn, E. V. Chulkov, S. Blugel, P. M. Echenique, and P. Hofmann, Phys. Rev. Lett. **93**, 196802 (2004).
[18] B. Weitzel and H. Micklitz, Phys. Rev. Lett. **66**, 385 (1991).
[19] T. E. Huber, A. Nikolaeva, D. Gitsu, L. Konopko, C. A. Foss, Jr., and M. J. Graf, Appl. Phys. Lett. **84**, 1326 (2004).
[20] L. Gammelgaard, J. W. Wells, K. Handrup, M. B. Balslev, J. E. Hansen, P. R. E. Petersen, P. Hofmann, and P. Bøggild, Appl. Phys. Lett. **93**, 093104 (2008).
[21] S. Hasegawa, I. Shiraki, F. Tanabe, R. Hobara, T. Kanagawa, T. Tanikawa, I. Matsuda, C. Petersen, T. Hansen, P. Boggild, and F. Gray, Surf. Rev. Lett. **10**, 963 (2003).
[22] T. Tanikawa, I. Matsuda, T. Kanagawa, and S. Hasegawa, Phys. Rev. Lett. **93**, 016801 (2004).
[23] J. W. Wells, J. F. Kallehauge, T. M. Hansen, and P. Hofmann, Phys. Rev. Lett. **97**, 206803 (2006).
[24] J. W. Wells, J. F. Kallehauge, and P. Hofmann, J. Phys.: Condens. Matter **19**, 176008 (2007).
[25] T. K. Kim, J. Wells, C. Kirkegaard, Z. Li, S. V. Hoffmann, J. E. Gayone, I. Fernandez-Torrente, P. Haberle, J. I. Pascual, K. T. Moore, A. J. Schwartz, H. He, J. C. H. Spence, K. H. Downing, S. Lazar, F. D. Tichelaar, S. V. Borisenko, M. Knupfer, and P. Hofmann, Phys. Rev. B **72**, 085440 (2005).
[26] J. E. Gayone, C. Kirkegaard, J. W. Wells, S. V. Hoffmann, Z. Li, and P. Hofmann, Appl. Phys. A: Mater. Sci. Process. **80**, 943 (2005).
[27] F. Smits, Bell Syst. Tech. J. **37**, 711 (1958).
[28] See http://www.capres.com for details of the probes.
[29] *CRC Handbook of Chemistry and Physics*, 80th ed., edited by D. Lide (CRC, Boca Raton, FL, 1999).
[30] J. P. Michenaud and J. P. Issi, J. Phys. C **5**, 3061 (1972).
[31] R. A. Hoffman and D. R. Frankl, Phys. Rev. B **3**, 1825 (1971).

[32]N. Garcia, Y. H. Kao, and M. Strongin, Phys. Rev. B **5**, 2029 (1972).
[33]T. Nagao, J. T. Sadowski, M. Saito, S. Yaginuma, Y. Fujikawa, T. Kogure, T. Ohno, Y. Hasegawa, S. Hasegawa, and T. Sakurai, Phys. Rev. Lett. **93**, 105501 (2004).
[34]T. Hirahara, I. Matsuda, C. H. Liu, R. Hobara, S. Yoshimoto, and S. Hasegawa, Phys. Rev. B **73**, 235332 (2006).
[35]T. Hirahara, T. Nagao, I. Matsuda, G. Bihlmayer, E. V. Chulkov, Y. M. Koroteev, and S. Hasegawa, Phys. Rev. B **75**, 035422 (2007).
[36]T. Hirahara, I. Matsuda, S. Yamazaki, N. Miyata, S. Hasegawa, and T. Nagao, Appl. Phys. Lett. **91**, 202106 (2007).